International Journal of Bifurcation and Chaos, Vol. 15, No. 8 (2005) 2559–2568

THE TRANSLINEAR PRINCIPLE: A GENERAL FRAMEWORK FOR IMPLEMENTING CHAOTIC OSCILLATORS

KOFI M. ODAME* and BRADLEY A. MINCH
School of Electrical and Computer Engineering,
Cornell University, Ithaca,
NY 14853-5401, USA
**kmo15@cornell.edu*

Received June 11, 2004; Revised July 29, 2004

In this Letter, we propose a class of nonlinear dynamic translinear circuits as a viable tool for the rapid and systematic implementation of chaotic oscillators in analog integrated circuits. In this regard, our primary focus is on multiple-input translinear element (MITE) networks and their particular merits. We also describe, as an illustrative example, our monolithic implementation of the Lorenz equations, and report on results from a test chip fabricated in a 0.5 μm CMOS process through MOSIS. We also show that Chua's circuit can be implemented easily in our framework.

Keywords: Multiple-input translinear element; chaotic attractor; Lorenz equations.

1. Introduction

The translinear principle is based on the Boltzmann distribution, and it essentially provides a simple, yet accurate, method for realizing product-of-power-law functions in analog circuits [Gilbert, 1996]. Dynamic translinear circuits exploit a generalization of this principle [Mulder *et al.*, 1997] to efficiently implement systems of ordinary differential equations of the form

$$\frac{dx_i}{dt} = f_i(\mathbf{x}), \quad i = 1, \ldots, n \tag{1}$$

where $\mathbf{x} = [x_1, x_2, \ldots, x_n]^T \in \mathbb{R}^n$, and the general form of $f_i(\mathbf{x})$ is

$$f_i(\mathbf{x}) = \sum_{k=1}^{N} \prod_{j=1}^{n} x_j^{\beta_j}, \quad \beta_j \in \mathbb{Q}. \tag{2}$$

From Eqs. (1) and (2), it is immediately apparent that dynamic translinear circuits may be used to implement a wide range of nonlinear dynamical systems, some of which exhibit chaos.

Chaotic behavior in integrated circuits has found applications in analog speech processing, in communication signal modulation, and in instrumentation [Delgado-Restituto & Rodriguez-Vazquez, 2002]. There is therefore keen interest in the question of designing analog VLSI circuits that exhibit chaos. Unfortunately, most of the published continuous-time CMOS chaotic oscillators are complex and large, and their realization demands a significant amount of design effort. One way to reduce the length of the design cycle is to create chaotic dynamical systems that are inherently well-suited to the current styles of circuit integration [Elwakil *et al.*, 2002]. Another approach — the one that we espouse — is to develop new, generalized methods for efficiently realizing chaotic analog circuits.

Elwakil and Kennedy [2000] contributed to the area by proposing a general description of chaotic oscillators. They conjectured that a chaotic oscillator is fundamentally composed of two blocks: a sinusoidal oscillator and a nonlinear resistor. While such an abstraction certainly illuminates the path

for the designer, there is still the question of how to implement a given nonlinearity in order to generate chaos.

Delgado-Restituto and Rodriguez-Vazquez [2002] discussed a general set of guidelines for the monolithic integration of chaotic oscillators that is centered around dimensionless state-space representation. Essentially, they present a toolbox of complex circuit blocks, each of which implements a particular mathematical function. The chaotic oscillator is pieced together by mapping each function in a given dynamical system's governing equations to its corresponding circuit block.

We too have adopted the state-space approach, but we do not make use of large, complicated functional blocks. Instead, what we propose is a concrete and complete synthesis methodology for the transistor-level implementation of any chaotic system whose dynamics are described by Eqs. (1) and (2). As we suggested above, our framework is based on the translinear principle. In particular, we will discuss the class of translinear circuits known as networks of multiple-input translinear elements (MITE).

Figure 1 shows the circuit symbol, and the most common physical realization, of the MITE. It consists of a floating gate MOSFET (FGMOS) and a cascode MOSFET. The FGMOS is the main component of the MITE, and it provides the following basic functions [Shibata & Ohmi, 1992]:

$$V_{\rm fG} = \sum_{j=1}^{n} w V_j, \tag{3}$$

and

$$\begin{aligned} I_{\rm D} &= I_{\rm s} e^{V_{\rm c}/U_{\rm T}} e^{V_{\rm fG}/U_{\rm T}} \\ &= I_{\rm s} e^{V_{\rm G}/U_{\rm T}}, \end{aligned} \tag{4}$$

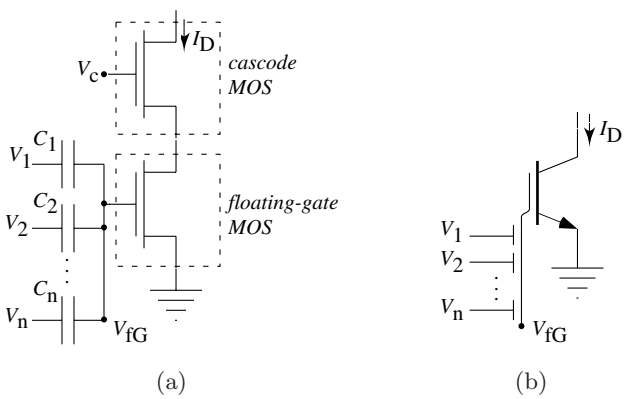

Fig. 1. Multiple-input translinear element: (a) practical implementation, and (b) circuit symbol.

where we have defined $V_{\rm G} = V_{\rm fG} + V_{\rm c}$. Here, $I_{\rm s}$ is a pre-exponential term that is largely dependent on the FGMOS transistor's geometry, $V_{\rm c}$ is the potential due to the charge on the floating gate, $U_{\rm T}$ is the thermal voltage and w is a weighting coefficients. The variables $V_1, \ldots, V_n$ are the *control-gate* voltages and $V_{\rm fG}$ is the *floating-gate* voltage. The drain current, $I_{\rm D}$, and the control-gate voltages $V_1, \ldots, V_n$ are the computational variables of the MITE; for a given computation, all of the other terms, such as $I_{\rm s}$ and w, are kept constant.

In the following sections, we will illustrate how these two basic functions, Eqs. (3) and (4) can be used to implement systems of differential equations.

2. The Lorenz Equations

To implement a chaotic system, such as the Lorenz equations, the idea is to first write the system in state-space form. Then, we can dimensionalize the equations, representing each state variable with whichever physical quantity is most convenient for our circuit implementation. For translinear circuit implementation, we represent each state variable by a current.

2.1. *Signed-value representation*

The standard representation of the Lorenz equations is already in state-space form, and is given by [Lorenz, 1963]

$$\begin{aligned} \dot{x} &= \sigma(y - x) \\ \dot{y} &= rx - y - xz \\ \dot{z} &= xy - bz. \end{aligned} \tag{5}$$

As mentioned earlier, the implementation of these equations requires that we represent each variable and parameter by an electrical current. Specifically, we will represent each variable and parameter by the drain current of a particular MITE. Notice from Eq. (4) that the MITE's drain current is given by $I_{\rm s}$ multiplied by an exponential function. $I_{\rm s}$ is a positive constant, and so the entire expression for the drain current must always be positive. This observation would imply that, in any equation that we attempt to implement as a MITE network, each variable must be one-sided; it is impossible for a drain current to directly represent a variable that can assume both positive and negative values. Of course, the Lorenz system is x- and y-symmetric, and so does not meet the one-sided restriction. We need to convert the system of

equations to an equivalent one that does meet this restriction, in order to make it implementable as a MITE network.

Our approach is to adopt a class-AB mode of operation, whereby variables are represented as the difference of two strictly positive, time-varying signals. For instance, we could write

$$\begin{aligned} x &= x_+ - x_- \\ y &= y_+ - y_- \\ z &= z_+ - z_-, \end{aligned} \tag{6}$$

where $(x_+, x_-), (y_+, y_-), (z_+, z_-)$ are pairs of positive, time-varying *differential* signal components.

We can differentiate Eq. (6) with respect to time to get

$$\begin{aligned} \dot{x} &= \dot{x}_+ - \dot{x}_- \\ \dot{y} &= \dot{y}_+ - \dot{y}_- \\ \dot{z} &= \dot{z}_+ - \dot{z}_-, \end{aligned} \tag{7}$$

and substitute into Eq. (5) to get

$$\begin{aligned} \dot{x}_+ - \dot{x}_- &= \sigma(y_+ - y_- - x_+ + x_-) \\ \dot{y}_+ - \dot{y}_- &= (x_+ - x_-)(r - z_+ + z_-) - y_+ + y_- \\ \dot{z}_+ - \dot{z}_- &= (x_+ - x_-)(y_+ - y_-) - b(z_+ - z_-). \end{aligned} \tag{8}$$

Now, we have got six variables, (x_+, x_-), (y_+, y_-) and (z_+, z_-), but only three equations. To keep the system of equations well-constrained, we must specify three more equations. Usually, each of the three extra equations defines the relationship between a pair of differential signal components. The geometric mean constraint is one such equation, which forces the product of two signals to approach some constant value. For the x-pair of signals, the geometric mean constraint is

$$\frac{d}{dt}(x_+ x_-) = q^2 - x_+ x_-, \tag{9}$$

where q^2 is the constant to which we would like $x_+ x_-$ to tend.

Applying the product rule to the LHS of Eq. (9) yields

$$\dot{x}_+ x_- + x_+ \dot{x}_- = q^2 - x_+ x_-,$$

which we can solve for $\dot{x}_+$ to find that

$$\dot{x}_+ = -x_+ + \frac{q^2}{x_-} - \frac{x_+ \dot{x}_-}{x_-}. \tag{10}$$

We can substitute this result into Eq. (8) and solve for $\dot{x}_+$ to get

$$\dot{x}_+ = \frac{x_+}{x_- + x_+}\left(-x_- + \frac{q^2}{x_+} + f(x,y,z)\right), \tag{11}$$

where we have defined $f(x, y, z) = \dot{x}$. More properly, we should have written $f(x_+ - x_-, y_+ - y_-, z_+ - z_-)$ in Eq. (11), but we will write $f(x, y, z)$ to avoid clutter.

If we apply the same geometric mean constraint to the y- and z-pairs, then, with analogous procedures, we can find expressions for all other differential signals and replace Eq. (5) with

$$\begin{aligned} \dot{x}_+ &= \frac{x_+}{x_- + x_+}\left(-x_- + \frac{q^2}{x_+} + f(x,y,z)\right) \\ \dot{x}_- &= \frac{x_-}{x_- + x_+}\left(-x_+ + \frac{q^2}{x_-} - f(x,y,z)\right) \\ \dot{y}_+ &= \frac{y_+}{y_- + y_+}\left(-y_- + \frac{q^2}{y_+} + g(x,y,z)\right) \\ \dot{y}_- &= \frac{y_-}{y_- + y_+}\left(-y_+ + \frac{q^2}{y_-} - g(x,y,z)\right) \\ \dot{z}_+ &= \frac{z_+}{z_- + z_+}\left(-z_- + \frac{q^2}{z_+} + h(x,y,z)\right) \\ \dot{z}_- &= \frac{z_-}{z_- + z_+}\left(-z_+ + \frac{q^2}{z_-} - h(x,y,z)\right), \end{aligned} \tag{12}$$

where $f(x, y, z)$, $g(x, y, z)$ and $h(x, y, z)$ are respectively the RHS of the $\dot{x}$, $\dot{y}$ and $\dot{z}$ equations in Eq. (5).

How can we be sure that each of the variables, x_+, x_-, y_+, y_-, z_+ and z_- will remain strictly positive? Well, if they are each represented by a drain current, then at least their initial values must be positive. From the continuity of the solutions, if x_+, say, ever became negative, then it would have to pass through zero. But, from Eq. (9), x_- would get arbitrarily large as x_+ got arbitrarily close to zero. Thus the difference, $x = x_+ - x_-$ will be a large, negative number. Since the solutions of the Lorenz equations are bounded, x cannot become arbitrarily large, and so x_+ must be bounded away from zero. The same is true for all of the other differential variables.

2.2. *Dimensionalization*

Because Eq. (12) satisfies the one-sided restriction, we can represent each variable by a drain current. We proceed with dimensionalization by replacing every variable and parameter in Eq. (12) with the ratio of a *signal* current to a *unit* current. The signal current is proportional to the dimensionless variable or parameter that it represents, and the unit current corresponds to unity. If we make the substitutions

Table 1. Current signal representations.

Dimensionless Term	Current Ratio
x_+	I_{x_+}/I_1
x_-	I_{x_-}/I_1
y_+	I_{y_+}/I_1
y_-	I_{y_-}/I_1
z_+	I_{z_+}/I_1
z_-	I_{z_-}/I_1
σ	I_σ/I_1
r	I_r/I_1
b	I_b/I_1
τ	I_τ/I_1

given in Table 1, Eq. (12) becomes

$$\begin{aligned}
\tau\frac{dI_{x_+}}{dt} &= \frac{I_{x_+}}{I_{x_+}+I_{x_-}}\left(-I_{x_-}+\frac{I_{\mathrm{q}}^2}{I_{x_+}}+f(\cdot)\right)\\
\tau\frac{dI_{x_-}}{dt} &= \frac{I_{x_-}}{I_{x_+}+I_{x_-}}\left(-I_{x_+}+\frac{I_{\mathrm{q}}^2}{I_{x_-}}-f(\cdot)\right)\\
\tau\frac{dI_{y_+}}{dt} &= \frac{I_{y_+}}{I_{y_+}+I_{y_-}}\left(-I_{y_-}+\frac{I_{\mathrm{q}}^2}{I_{y_+}}+g(\cdot)\right)\\
\tau\frac{dI_{y_-}}{dt} &= \frac{I_{y_-}}{I_{y_+}+I_{y_-}}\left(-I_{y_+}+\frac{I_{\mathrm{q}}^2}{I_{y_-}}-g(\cdot)\right)\\
\tau\frac{dI_{z_+}}{dt} &= \frac{I_{z_+}}{I_{z_+}+I_{z_-}}\left(-I_{z_-}+\frac{I_{\mathrm{q}}^2}{I_{z_+}}+h(\cdot)\right)\\
\tau\frac{dI_{z_-}}{dt} &= \frac{I_{z_-}}{I_{z_+}+I_{z_-}}\left(-I_{z_+}+\frac{I_{\mathrm{q}}^2}{I_{z_-}}-h(\cdot)\right)
\end{aligned} \tag{13}$$

2.3. *Product-of-power-law functions*

Now let us concentrate on implementing the first of these six equations. After fully expanding it, the RHS becomes

$$\begin{aligned}
\tau\frac{dI_{x_+}}{dt} = \frac{I_{\mathrm{q}}^2}{I_{x_+}+I_{x_-}} &- \frac{I_{x_+}I_{x_-}}{I_{x_+}+I_{x_-}}\\
&+\frac{I_{x_+}I_\sigma I_{y_+}}{I_1(I_{x_+}+I_{x_-})}-\frac{I_{x_+}I_\sigma I_{y_-}}{I_1(I_{x_+}+I_{x_-})}\\
&+\frac{I_{x_+}I_\sigma I_{x_-}}{I_1(I_{x_+}+I_{x_-})}-\frac{I_{x_+}I_\sigma I_{x_+}}{I_1(I_{x_+}+I_{x_-})}
\end{aligned} \tag{14}$$

Each term on the RHS, for instance $I_{x_+}I_{x_-}/(I_{x_+}+I_{x_-})$, has got the general form of a multiply/divide function. We will presently describe how a *MITE network* can implement a multiply/divide function.

We define a set of MITEs as a MITE network if each MITE has got at least one control-gate that is in electrical contact with another MITE in the set, and if, regarding the MITEs as nodes and the electrical contacts between control-gates as edges, the set of MITEs forms a connected graph. Figure 2 shows a simple example of a MITE network. Applying Eq. (3) to each MITE's floating-gate, we get the following set of simultaneous equations:

$$\begin{aligned}
V_{\mathrm{f0}} &= 2wV_0\\
V_{\mathrm{fa}} &= wV_0+wV_1\\
V_{\mathrm{fb}} &= wV_1+wV_2\\
V_{\mathrm{fc}} &= wV_2+wV_3\\
V_{\mathrm{fout}} &= wV_3+wV_0.
\end{aligned} \tag{15}$$

We can express V_{fout} in terms of the other floating-gate voltages as

$$V_{\mathrm{fout}} = V_{\mathrm{fa}} - V_{\mathrm{fc}} + V_{\mathrm{fb}}, \tag{16}$$

To find an expression for I_{out}, we substitute Eq. (16) into Eq. (4) to get

$$\begin{aligned}
I_{\mathrm{out}} &= I_{\mathrm{s}}e^{V_{\mathrm{c}}/U_{\mathrm{T}}}e^{(V_{\mathrm{fa}}-V_{\mathrm{fc}}+V_{\mathrm{fb}})/U_{\mathrm{T}}}\\
&= \frac{I_{\mathrm{s}}e^{V_{\mathrm{c}}/U_{\mathrm{T}}}e^{V_{\mathrm{fa}}/U_{\mathrm{T}}}\cdot I_{\mathrm{s}}e^{V_{\mathrm{c}}/U_{\mathrm{T}}}e^{V_{\mathrm{fb}}/U_{\mathrm{T}}}}{I_{\mathrm{s}}e^{V_{\mathrm{c}}/U_{\mathrm{T}}}e^{V_{\mathrm{fc}}/U_{\mathrm{T}}}} = \frac{I_{\mathrm{a}}I_{\mathrm{b}}}{I_{\mathrm{c}}}.
\end{aligned} \tag{17}$$

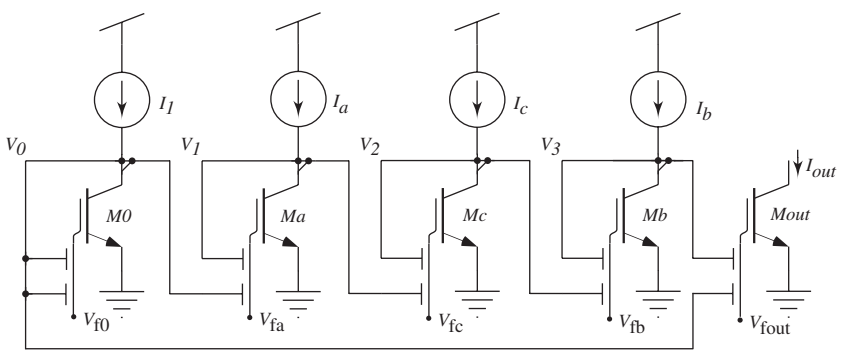

Fig. 2. A network of MITEs.

Equation (17) shows that MITE networks are capable of implementing multiply/divide functions. We recently gave a constructive proof of the fact that the more general class of product-of-power-law functions,

$$p(\boldsymbol{x}) = \prod_{j=1}^{n} x_j^{\beta_j}, \quad \beta_j \in \mathbb{Q}, \tag{18}$$

is readily implementable by a network of MITEs [Minch, 2003].

Notice that the terms in the RHS of Eq. (14) do not have the exact form of a product-of-power-law function, since their denominators contain an addition, $I_{x_+} + I_{x_-}$. However, we can easily rectify this by defining $I_{xs} = I_{x_+} + I_{x_-}$, and rewriting Eq. (14) as

$$\tau \frac{dI_{x_+}}{dt} = \frac{I_{x_+} I_{x_-}}{I_{xs}} - \frac{I_{\mathrm{q}}^2}{I_{xs}} + \frac{I_{x_+} I_\sigma I_{y_-}}{I_1 I_{xs}} - \frac{I_{x_+} I_\sigma I_{y_+}}{I_1 I_{xs}} + \frac{I_{x_+} I_\sigma I_{x_+}}{I_1 I_{xs}} - \frac{I_{x_+} I_\sigma I_{x_-}}{I_1 I_{xs}}. \tag{19}$$

Figure 3(a) shows how to implement I_{xs} in a MITE network: by Kirchhoff's current law (KCL), $I_{xs} = I_{x_+} + I_{x_-}$ is generated when two wires, one carrying I_{x_+}, and the other carrying I_{x_-}, are connected together.

The RHS of Eq. (19) is itself the summation and subtraction of several of the product-of-power-law terms. As Figs. 3(b) and 3(c) show, we can again apply KCL to achieve these additions and subtractions. For instance, to add, we just connect the outputs of two MITE networks to a single wire. To subtract, we use a current mirror to reverse the direction of one of the outputs, and then add it to the other output. Thus, we have taken care of implementing the RHS of Eq. (19).

2.4. *Time derivatives*

In this subsection, we will discuss how to implement the LHS of Eq. (19), namely the time derivative. We again turn to the MITE's basic functions of summation and exponentiation [Mulder *et al.*, 1997; Minch, 2004]. We can substitute Eq. (3) into Eq. (4), and differentiate with respect to time, via the chain rule, to obtain

$$\frac{dI_{\mathrm{D}}}{dt} = \sum_{j=1}^{n} \left(\frac{\partial I_{\mathrm{D}}}{\partial V_j} \frac{dV_j}{dt} \right) = I_{\mathrm{D}} \sum_{j=1}^{n} \left(\frac{w_j}{U_{\mathrm{T}}} \frac{dV_j}{dt} \right) \tag{20}$$

Multiplying top and bottom of the RHS of Eq. (20) by *integrator* capacitances, C_i, yields

$$\frac{dI_{\mathrm{D}}}{dt} = I_{\mathrm{D}} \sum_{i=1}^{n} \left(\frac{w_i}{C_i U_{\mathrm{T}}} \cdot C_i \cdot \frac{dV_i}{dt} \right). \tag{21}$$

Next, we multiply both sides of Eq. (21) by the characteristic time scale, τ, to get

$$\tau \frac{dI_{\mathrm{D}}}{dt} = I_{\mathrm{D}} \sum_{i=1}^{n} \left(\frac{\tau w_i}{C_i U_{\mathrm{T}}} \cdot C_i \cdot \frac{dV_i}{dt} \right). \tag{22}$$

As it turns out, we can interpret each $C_i dV_i/dt$ term as a (capacitor) current, I_{Ci}. Also, each of the terms $C_i U_{\mathrm{T}}/\tau w_i$ has units of charge per second, and so is essentially a current, which we will call $I_{\tau i}$. Thus, we can express the time derivative of a MITE's output current as

$$\tau \frac{dI_{\mathrm{D}}}{dt} = I_{\mathrm{D}} \sum_{i=1}^{n} (I_{Ci} I_{\tau i}^{-1}). \tag{23}$$

Note that the control-gate voltages, V_i, do not all have to be time-varying. If we hold constant all the control-gate voltages except for V_1, we get, for $i \neq 1$,

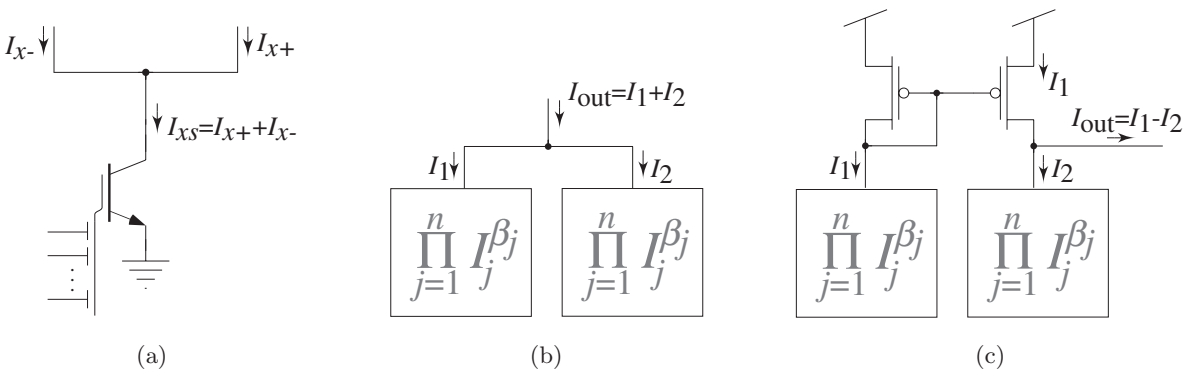

Fig. 3. Using KCL to implement (a) $I_{xs} = I_{x_+} + I_{x_-}$, (b) summation, and (c) subtraction of product-of-power-law functions.

$C_i dV_i/dt = I_{Ci} = 0$, which means we can write

$$\tau \frac{dI_{\mathrm{D}}}{dt} = \frac{I_{\mathrm{D}} I_{C1}}{I_{\tau 1}}. \tag{24}$$

We can now write Eq. (19) as

$$I_C = \frac{I_\tau I_{x-}}{I_{x\mathrm{s}}} - \frac{I_\tau I_{\mathrm{q}}^2}{I_{x+} I_{x\mathrm{s}}} + \frac{I_\tau I_\sigma I_{y-}}{I_1 I_{x\mathrm{s}}} - \frac{I_\tau I_\sigma I_{y+}}{I_1 I_{x\mathrm{s}}} + \frac{I_\tau I_\sigma I_{x+}}{I_1 I_{x\mathrm{s}}} - \frac{I_\tau I_\sigma I_{x-}}{I_1 I_{x\mathrm{s}}}. \tag{25}$$

I_τ is simply a constant current which we choose, in conjunction with the integrator capacitance size, C, to set an appropriate value for the time-constant, τ.

In general, take an n-input MITE, with $n-1$ of the control-gates held at fixed voltages. If the MITE's drain current, I_{D}, is time-varying, then this must be due solely to voltage changes in the last remaining control-gate. If we can convert the time-derivative of this control-gate's voltage to a current, via $C\dot{V} = I_C$, then the time-derivative of the MITE's drain current, $\dot{I}_{\mathrm{D}}$, is directly proportional to $I_{\mathrm{D}} I_C / I_\tau$. We have already seen how a MITE network can implement such a multiply/divide function. We can go through similar processes for the other five equations, thereby implementing the entire Lorenz system. (See [Odame, 2004] for a detailed description of the circuit implementation.) In fact, the synthesis methodology can be used to implement any differential equation of the form $dI/dt = F(\cdot)$, where $F(\cdot)$ is a sum of product-of-power-law functions. (Polynomial differential equations are one obvious subset of this class of functions.) The resulting circuit has got no resistors or inductors, and so it is highly amenable to integration. There are no complex functional blocks, such as opamps or filters, and so the design is very compact.

3. Results

Figure 4 shows a micrograph of the monolithic Lorenz implementation, fabricated in a 0.5 µm AMI process from MOSIS. Because we used such a simple element as the MITE to carry out most of the computation, our design resulted in the regularly-structured, tightly-packed array that Fig. 4 depicts. The bounding box around the circuit, including integrator-capacitors, is 0.7 mm^2. The circuit runs on a single-ended 3 V supply, and dissipates less than 20 mW of power.

In order to measure the circuit's output on an oscilloscope, we converted the MITE network's current signals into voltages, using off-chip transimpedance amplifiers made from discrete parts on a protoboard. Figure 5 is a time series graph of the voltages that correspond to the I_{x+}, I_{y+} and I_{z+} signals, when the system is exhibiting chaos. The graph shows that each signal oscillates on the positive and negative sides, and, at least for the window of time that we observe, there is no discernible periodicity. Our measurements suffered from the additional pin parasitics of the extra IC's that make up the transimpedance amplifiers, as well as from large area wire loops between the test circuit and the amplifiers. If we were to integrate the transimpedance amplifiers on chip, we would probably eliminate the noise that is superimposed on the waveforms shown in Fig. 5. The trajectory of Fig. 5 has got a correlation dimension [Grassberger & Procaccia, 1983] given by Fig. 6 as $D_c \approx 2.06$, which matches favorably with the usual value of about 2.05. Figure 7 is a projection of the trajectory onto the x–z plane, and it depicts the familiar butterfly-wings of the Lorenz attractor.

The highest frequency content of the circuit was measured to be roughly 10 kHz. The frequency of the circuit is primarily limited by the particular implementation of MITEs that we used, which

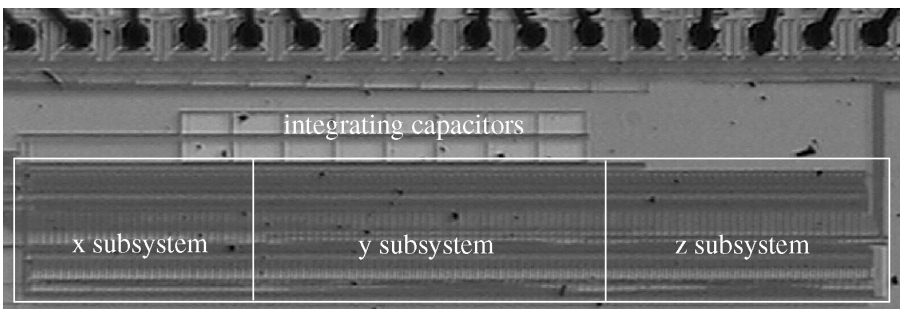

Fig. 4. Micrograph of Lorenz system.

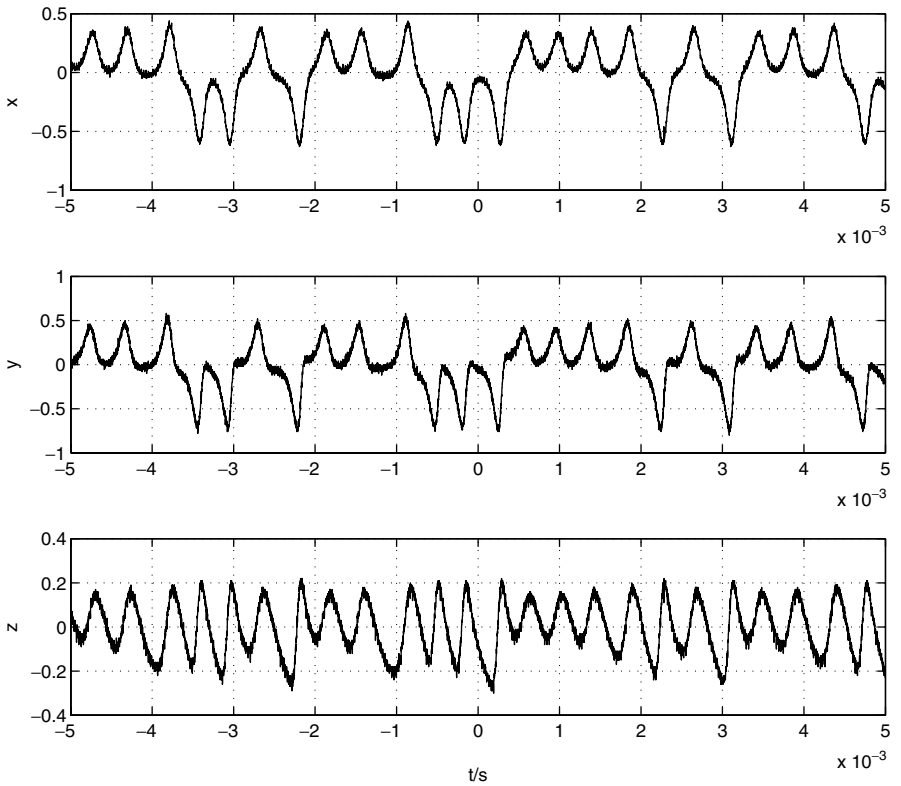

Fig. 5. Time series graphs of voltages corresponding to I_{x_+}, I_{y_+}, I_{z_+} signals.

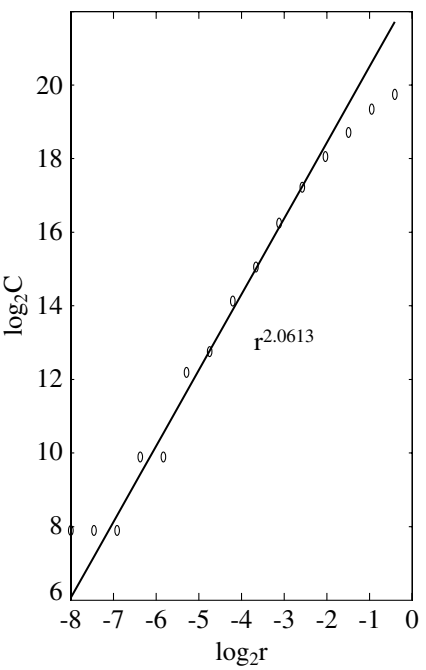

Fig. 6. Correlation dimension of Lorenz attractor; $D_c \approx 2.06$.

Fig. 7. Projection of chaotic attractor onto x–z plane.

operate on low, subthreshold currents. We have proposed various alternatives to this conventional MITE implementation, two of which allow for the use of bipolar junction transistors (BJTs) in place of subthreshold MOSFETs [Minch *et al.*, 1998; Odame *et al.*, 2003]. BJTs permit operation of the circuit at currents that are much higher than subthreshold, thus yielding higher bandwidths. Using

standard CMOS technology, we can implement a type of BJT known as the complementary lateral bipolar transistor [Vittoz, 1983], which should allow us to scale the frequency of the circuit at least into the MHz range. In a BiCMOS process with one flavor of SiGe HBTs, there is no reason that the circuit should not go into the 100s of MHz to GHz range.

4. Eliminating Nonideal Effects

4.1. *Transistor mismatch*

One limiting factor to analog circuit performance is the mismatch of nominally-identical devices. Despite very tightly-controlled manufacturing processes, nominally-identical devices fabricated on the same chip will have slightly different behaviors. With regard to MITEs, this deviation is largely manifested in a scaling of the drain current. For the ith MITE on a chip, Eq. (4) must be rewritten as

$$\begin{aligned} I_{\mathrm{D}} &= \alpha_i I_{\mathrm{s}} e^{(V_{\mathrm{c}}/U_{\mathrm{T}})} e^{V_{\mathrm{fG}}/U_{\mathrm{T}}} \\ &= \alpha_i I_{\mathrm{s}} e^{V_{\mathrm{G}}/U_{\mathrm{T}}}, \end{aligned} \tag{26}$$

where $\alpha_i \in \mathbb{R}^+$ depends on the MITE in question. If we accounted for α_i in our analysis of Fig. 2, we would find that the MITE network implemented

$$I_{\mathrm{out}} = \frac{\alpha_{\mathrm{out}}\alpha_{\mathrm{c}}}{\alpha_{\mathrm{a}}\alpha_{\mathrm{b}}} \frac{I_{\mathrm{a}} I_{\mathrm{b}}}{I_{\mathrm{c}}}, \tag{27}$$

which is still a multiply/divide function, but with an uncontrollable gain factor. Similarly, any attempt to implement a product-of-power-law function with a MITE network would result in a function that had an uncontrollable gain factor.

Fortunately, we have a means of nullifying the effect of the α_i term. Under normal operation, the charge on the floating gate, V_{c}, is nonvolatile, and should remain constant indefinitely. However, the quantum-mechanical phenomena of *Fowler–Nordheim tunneling* and *hot-electron injection* allow us to vary the amount of charge on the floating-gate. Using a scheme similar to that described in [Kucic *et al.*, 2001], we have very precise control on the value of V_{c}. In particular, for any α_i, we can choose $V_{\mathrm{c}} = -U_{\mathrm{T}} \log(\alpha_i)$, so that Eq. (26) becomes

$$I_{\mathrm{D}} = I_{\mathrm{s}} e^{V_{\mathrm{fG}}/U_{\mathrm{T}}}. \tag{28}$$

The significance of Eq. (28) is that we can program all of the MITEs such that, for a given value of $V_{\mathrm{fG}} = \sum_{j=1}^{n} w V_j$, they each pass the same drain current. From this standpoint, the MITEs are effectively identical to each other. If we analyze Fig. 2 with Eq. (28), it is straight forward to see that the pure multiply/divide function, Eq. (17), still holds. Also, the MITE network implementations of product-of-power-law functions are free of this particular gain error, when the MITEs' floating-gate charges are programmed to ensure that $V_{\mathrm{c}} = -U_{\mathrm{T}} \log(\alpha_i)$.

4.2. *Integrator capacitor mismatch*

We mentioned earlier that the time-constant, τ, in a MITE network implementation of a differential equation is directly proportional to the size of the integrator capacitor. From Eqs. (22) and (23), the relationship is

$$\tau = \frac{C U_{\mathrm{T}}}{I_\tau w}, \tag{29}$$

where U_{T} and w are defined as before, and I_τ is a constant current.

The capacitance of an integrator capacitor is determined by its physical geometry and so its precise value is subject to the vagaries of the fabrication process, varying by as much as 1% from its nominal value. The value of C in Eq. (29) might be controllable to only a few percent, but it is still possible to regulate the value of τ fairly tightly. The current I_τ is a tunable parameter, and we are free to adjust it, according to the actual values of C, w and U_{T}, in order to achieve the desired τ.

5. Chua's Circuit

Because of its popularity and rich dynamical behavior, we find it worthwhile to briefly consider the implementation of Chua's circuit, and to show how it too is easily realizable as a dynamic MITE network.

The governing equations for Chua's circuit [Matsumoto *et al.*, 1985] are

$$\begin{aligned} C_1 \frac{dV_{C1}}{dt} &= G(V_{C2} - V_{C1}) - g(V_{C1}) \\ C_2 \frac{dV_{C2}}{dt} &= G(V_{C1} - V_{C2}) + i_L \\ L \frac{di_L}{dt} &= -V_{C2}, \end{aligned} \tag{30}$$

where V_{C1}, V_{C2} are time-varying voltages and i_L is a time-varying current. C_1, C_2, L and G are parameters, and $g(V_{C1})$ is a piecewise-linear

function given by

$$g(V_{C1}) = m_0 V_{C1} + \frac{(m_0 - m_1)}{2}|V_{C1} + B_p| + \frac{(m_1 - m_0)}{2}|V_{C1} - B_p|, \quad (31)$$

with variables m_0, m_1 and B_p. The state-space decomposition of Eq. (30) is

$$\begin{aligned} \dot{x} &= \alpha\left(y - x - bx + \frac{b-a}{2}(|x+E| - |x-E|)\right) \\ \dot{y} &= x - y + z \\ \dot{z} &= -\beta y, \end{aligned} \quad (32)$$

where x, y and z are state variables, and α, β, a, b and E are parameters [Rodriguez-Vazquez & Delgado-Restituto, 1993].

To synthesize a MITE network that implements Eq. (32), the idea is to again dimensionalize the equations, and to express the RHS as sums of product-of-power-law functions. The only parts of Eq. (32) whose MITE implementation might not be directly obvious are the absolute-value functions that describe the Chua's diode. We will therefore demonstrate how to implement, say,

$$u = |x + E|. \quad (33)$$

Squaring both sides of Eq. (33) yields

$$u^2 = (x+E)^2 = x^2 + 2xE + E^2. \quad (34)$$

We can assume that the state variable x is represented differentially, by $x = x_+ - x_-$. In that case, Eq. (34) becomes

$$\begin{aligned} u^2 &= (x_+ - x_-)^2 + 2(x_+ - x_-)E + E^2 \\ &= x_+^2 - 2x_+x_- + x_-^2 + 2x_+E - 2x_-E + E^2. \end{aligned} \quad (35)$$

To dimensionalize, we apply the following substitutions

$$u = \frac{I_u}{I_1},$$

$$x_+ = \frac{I_{x_+}}{I_1},$$

$$x_- = \frac{I_{x_-}}{I_1},$$

$$E = \frac{I_E}{I_1},$$

to Eq. (35) to get

$$I_u^2 = I_{x_+}^2 - 2I_{x_+}I_{x_-} + I_{x_-}^2 + 2I_{x_+}I_E - 2I_{x_-}I_E + I_E^2. \quad (36)$$

Now, if we define

$$I_v I_1 = I_{x_+}^2 - 2I_{x_+}I_{x_-} + I_{x_-}^2 + 2I_{x_+}I_E - 2I_{x_-}I_E + I_E^2,$$

then we can write

$$I_v = \frac{I_{x_+}^2}{I_1} - \frac{2I_{x_+}I_{x_-}}{I_1} + \frac{I_{x_-}^2}{I_1} + \frac{2I_{x_+}I_E}{I_1} - \frac{2I_{x_-}I_E}{I_1} + \frac{I_E^2}{I_1} \quad (37)$$

and

$$I_u = (I_v I_1)^{1/2}. \quad (38)$$

Equation (37) is a sum of product-of-power-law functions, and so is directly implementable by applying KCL to the outputs of a few MITE networks. Equation (38) is a product-of-power-law function, and is also implementable as a MITE network. Note that, since I_u is a drain current, it can only take the positive root of $I_v I_1$, and so Eqs. (38) and (37) together represent a correct physical realization of the absolute-value function, Eq. (33). If we apply the same procedure to $|x - E|$, we find that the entire RHS of Eq. (32) is nothing more than sums of product-of-power-law functions, and is therefore directly implementable as MITE network.

6. Conclusion

We have presented translinear circuit design as a general framework for implementing chaotic oscillators in analog VLSI. Our methodology was illustrated by the implementation of the Lorenz system as a MITE network. We supported our discussion by presenting experimental results, which verified that the resulting analog circuit is a functional representation of the Lorenz equations. Finally, we showed that Chua's circuit should just as easily be implemented as a MITE network.

References

Delgado-Restituto, M. & Rodriguez-Vazquez, A. [2002] "Integrated chaos generators," in *Proc. IEEE*, Vol. 90, pp. 747–767.

Elwakil, A. S. & Kennedy, M. P. [2000] "Chua's circuit decomposition: A systematic design approach for autonomous chaotic oscillators," *J. Franklin Instit.* **337**, 251–265.

Elwakil, A. S., Salama, K. N. & Kennedy, M. P. [2002] "An equation for generating chaos and its monolithic implementation," *Int. J. Bifurcation and Chaos* **12**, 2885–2958.

Gilbert, B. [1996] "Translinear circuits: An historical review," *Anal. Integr. Circuits Sign. Process.* **9**, 95–118.

Grassberger, P. & Procaccia, I. [1983] "Characterization of strange attractors," *Phys. Rev. Lett.* **50**, 346–349.

Kucic, M., Hasler, P., Dugger, J. & Anderson, D. [2001] "Programmable and adaptive analog filters using arrays of floating-gate circuits," in *Proc. Advanced Research in VLSI*, *ARVLSI'01*, pp. 148–162.

Lorenz, E. N. [1963] "Deterministic non-periodic flow," *J. Atmos. Sci.* **20**, 130–141.

Matsumoto, T., Chua, L. & Komuro, M. [1985] "The double scroll," *IEEE Trans. Circuits Syst.* **32**, 797–818.

Minch, B. A., Hasler, P. & Dioro, C. [1998] "The multiple-input translinear element: A versatile circuit element," in *Proc. ISCAS'98*, Vol. 1, pp. 527–530.

Minch, B. A. [2003] "Construction and transformation of multiple-input translinear element networks," *IEEE Trans. Circuits Syst.-I* **50**, 1530–1537.

Minch, B. A. [2004] "Synthesis of static and dynamic multiple-input translinear element networks," *IEEE Trans. Circuits Syst.-I* **51**, 409–421.

Mulder, J., Van der Woerd, A. C., Serdijn, W. A. & Van Roermund, A. H. M. [1997] "An RMS-DC converter based on the dynamic translinear principle," *IEEE J. Solid-State Circuits* **32**, 1146–1150.

Odame, K. [2004] *A Multiple-Input Translinear Element Network Implementation of the Lorenz Equations*, M.S. thesis, Cornell University.

Odame, K. M., McDonald, E. J. & Minch, B. A. [2003] "Highly linear, wide-dynamic-range multiple-input translinear element networks," in *Proc. Asilomar Conf. Signals, Systems and Computers*, *ASILOMAR'03*, Vol. 2, pp. 2036–2040.

Rodriguez-Vazquez, A. & Delgado-Restituto, M. [1993] "CMOS design of chaotic oscillators using state variables: A monolithic Chua's circuit," *IEEE Trans. Circuits Syst.-II* **40**, 596–613.

Shibata, T. & Ohmi, T. [1992] "A functional MOS transistor featuring gate-level weighted sum and threshold operations," *IEEE Trans. Electron Dev.* **39**, 1444–1455.

Vittoz, E. A. [1983] "MOS transistors operated in the lateral bipolar mode and their application in CMOS technology," *IEEE J. Solid-State Circuits* **18**, 273–279.